



## Amplification Loop for Laser Mirror Techniques for Deep Learning

<sup>1</sup> Haider Yahya saeed, <sup>2</sup> Husam Noman MohammedAli, <sup>3</sup> Ali Abdul Abas Al Bakri<sup>4</sup> Haidar Zaeer Dhaam

<sup>1</sup>Msc, <sup>2</sup>doc, <sup>3</sup>prof, <sup>4</sup>Mrs

<sup>1</sup> Communications Tech. Eng,

<sup>1</sup> Al-Furat Al-Awsat Technical University (ATU), Najaf, Iraq.

**Abstract :** Many researchers have identified the fundamental challenge in these types of systems, which is nonlinearity of the amplification properties; one solution for this critical issue is to use delearniep ng and evolutionary searching algorithms. The primary evolutionary algorithm and the optical simulation model are given in this study, along with simulation data, to tackle this challenge.

### INTRODUCTION

While method-locked lasers are a well-established knowledge with multiple uses in commerce, medication, and metrology, they also include a significant body of basic and applied research. Fundamentally, mode-locked lasers are a good platform for the research of innovative and difficult concepts. ultrashort pulses' nonlinear dynamics [1-3]. At the applied level, pulses with optimal characteristics—for example, in terms of the basic limitation of developing efficient pulse length, energy, repetition rate, and radiation bandwidth cavity architectures— are utilized. In both of these categories, fiber lasers are superior. Cavities, which offer a small and multipurpose design, are an example from a rapidly developing area [4]. The relationship between the PC configuration and the nonlinear transfer function, on the other hand, is a major issue [5,6], The presence of lump refraction effects in fiber laser trial configurations exacerbates this problem [7]. As a result, in most evaluation, the experimentalist manually twists the integrated PCs' three or four holds in a trial-and-error technique, hoping to achieve stable mode locking among a huge variety of pulse dynamically efficient cavity topologies, for example. The gain-adjustable nonlinear amplifying loop mirror (NALM) has a cubic significant dependency based on a low-energy input pulse and intermediate values, leading in excellent background suppression and a minor reduction in pulse interactions [8]. Because to its operation strategy reflectivity, the NALM provides an extra pulse shaping mechanism [9]. [10] and [11] Early-stage thulium-doped mode-locked fiber lasers with intracavity dispersion management based on both lined and loop cavity topologies were demonstrated. The shortest pulse duration was achieved by using precise intracavity dispersion control of two hundred and twenty five (fs) and spectral bandwidth of twenty two( nm) with twenty (mW) average output power were obtained [9].

Table (1)In the literature review, we listed all of the experimental laser fiber double gain cavity nonlinear setups as well as all of the proposed modeling.

**Table(1): Illustration of all literature schematic diagram**

No.	References	Experimental setup (schematic diagram)
1	Maria A. Chernysheva, and at el, 2012,[12]	<p>Figure 1: mirror loop for double gain laser fiber optics.</p>

2 Yi-Jing You, 2015,[13].

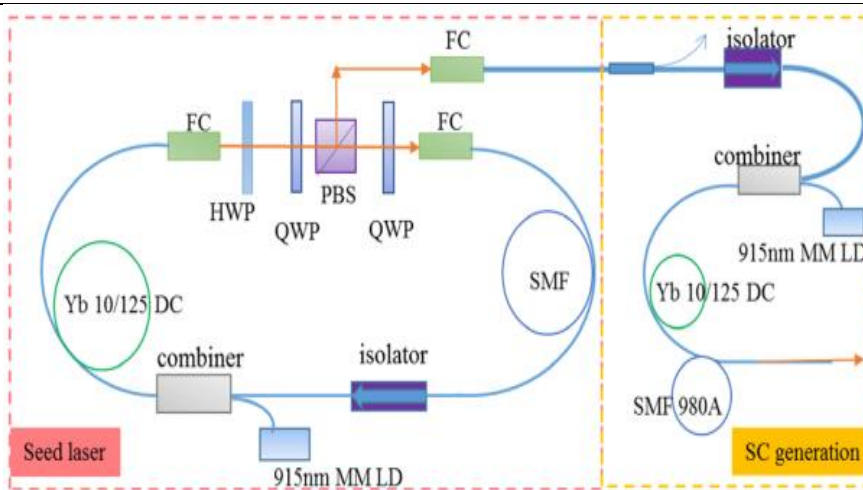


Figure 2: Schematic diagram for combiner fiber optics laser loop.

3 U. ANDRAL, 2015,[14].

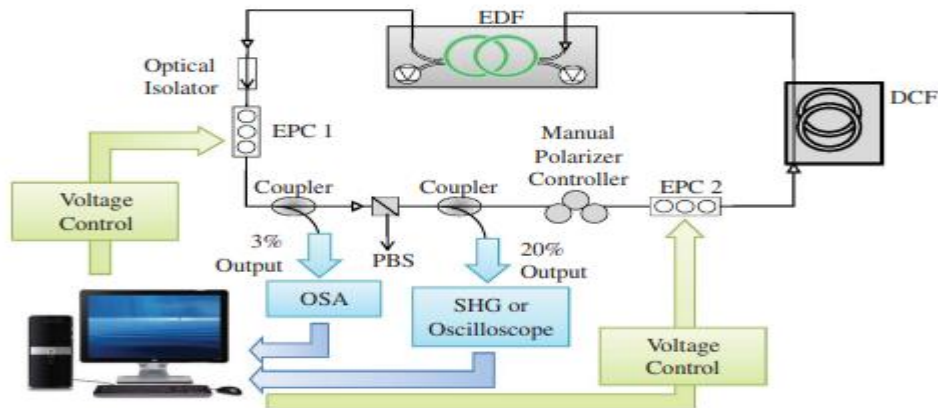


Figure 3: schematic diagram of the experimental setup for double band mirror loop.

4 Sonio Basclon, et al, 2019,[15]

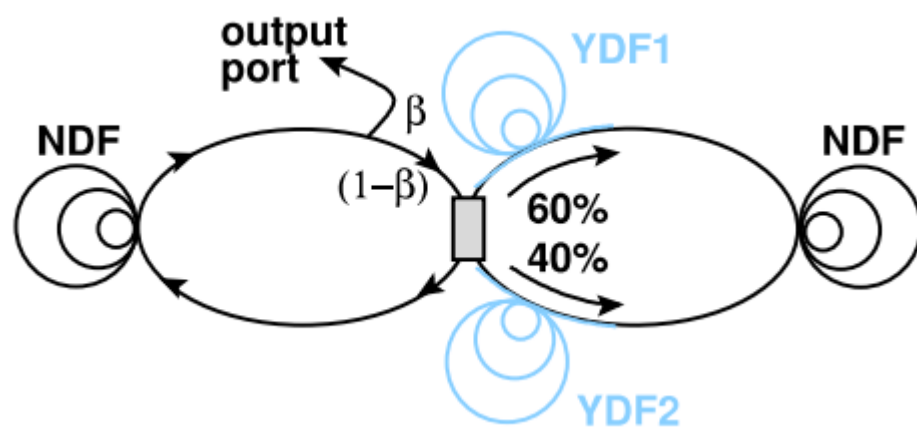


Figure 4: schematic diagram of the experimental setup that has adaptive from ref[15].

We use Machine Learning (ML) methods, Particle Swarm Optimization (PSO) methods, and Genetic Algorithms .For the first time, we were able to efficiently regulate the commencement of nonlinear dynamics of optical emission in the laser cavity and create pulsed regimes with varied duration, energy, optical spectrum width, two electronic-managed distributed gain parameters, and degree of coherence We provide a set of objective functions that allow us to generate on-demand pulses with the shortest

length, maximum energy, and cohesive variability. The application of algorithmic, electronically-driven control over emission method-locking systems adds to the adaptability of the proposed laser approach.

## 2. Machine learning techniques:

In this section, we've discussed two key evolution strategies that have been employed in the literature, as well as a proposed method

### 2.1 Genetic algorithm:

Figure 5 depicts the schematics of the genomic algorithm used in this investigation. The "individual" of a populace is a pulsed system containing two genes – the values of the two pushing diode currents. The compare of the radio frequency (RF) spectrum of the basic mode, the middle power, the period of the autocorrelation purpose, and the compare of the coherence spine are all unique to each person. These numbers can be used to create a fitness function, which a genomic algorithm will try to optimize. The maximum value of the objective (fitness) function corresponds to the pulsed system with the required parameters. The genomic algorithm starts by randomly seeding the population with two currents. As a result, each number is a multiple of 0 and 1. After sorting the population by the fitness function's value, individuals are mated by mixing their genes at random. The elite group of people with the greatest fitness function scores remains stable. A segment of the populace is changed by change, which is a random conversion of genes, to avoid the fitness function's local maximum being clamped by the algorithm. The algorithm rotation can be halted if the change in the objective function remains smaller than a threshold value throughout numerous rotation. In order for the algorithm to work, the population size, the percentage of elite people, and the percentage of mutant people must all be supplied.

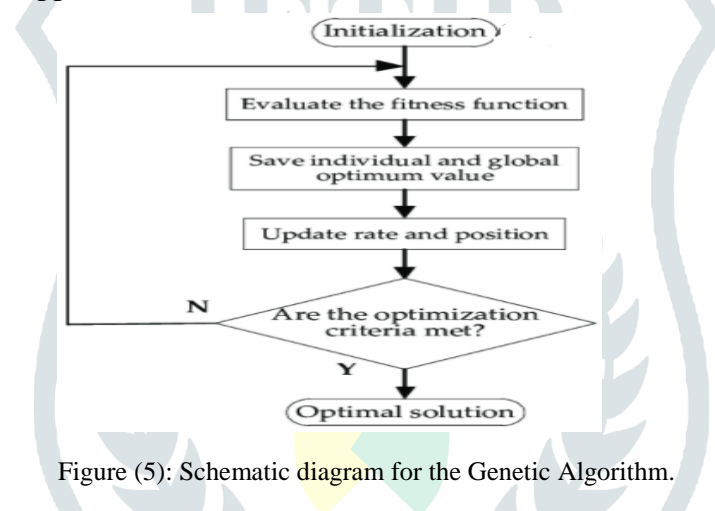


Figure (5): Schematic diagram for the Genetic Algorithm.

### 2.2 Particle swarm optimization algorithm:

At the center of our research is the application of the particle swarm optimization method to the inverse design of the examined laser system in the shape of an eight. The gradient-free particle swarm optimization (PSO) algorithm was used to map the desired attributes of the laser's output pulses with the laser's parameters a figure-eight pattern cavity. The procedure starts with a chance initialization of (N) swarm particles with locations and velocities. A particle's position is a vector of cavity parameters in our scenario, and velocity controls how this vector changes in the next stage of the algorithm. We use a (NLSE) based model of an figure-eight pattern fiber laser to simulate pulse generation for each particle. The fitness function is then applied to the particles in order to determine how close they are to the target pulse.

$$\mathbf{v}_i \leftarrow \omega \mathbf{v}_i + \phi_p \mathbf{r}_p \times (\mathbf{p}_i - \mathbf{x}_i) + \phi_g \mathbf{r}_g \times (\mathbf{p}_g - \mathbf{x}_i),$$

where  $\mathbf{x}_i$  is the stream set of parameters for the (i-th) particle, ( $\mathbf{p}_i$ ) is the previous highest ranking of the (i-th) particle, and  $\mathbf{p}_g$  is the previous best position of the entire group,  $\mathbf{r}_p$ ,  $\mathbf{r}_g$  are random values that update each iteration step between zero and one, and  $\phi_p$ ,  $\phi_g$  are hyperparameters that influence convergence speed. The "Method" section describes the hyperparameters' precise values. The method is repeated until the fitness function reaches a target edge value or the conversion in the fitness function does not exceed the corresponding variation edge level. The fitness functions' goal is to determine the desired output pulses (targeted). It was constructed with parameters that are regularly used in practice in this example: e For each phase, utilizing the temporal and spectral distributions' Full-width half maximum (FWHM)

$$f(\Delta T, \Delta \lambda) = \alpha_1 \cdot \frac{|\Delta T - \Delta T_{target}|}{T_{max}} + \alpha_2 \cdot \frac{|\Delta \lambda - \Delta \lambda_{target}|}{\lambda_{max}},$$

$T_{max}$  and  $\max$  are the widths of the numerical model's temporal and spectral windows,  $T$  is the target, and target are desirable values, 1 and 2 are temporal and spectral weights, and  $T_{max}$  and  $\max$  are the widths of the numerical model's temporal and spectral windows. It's worth noting that, as shown in figure 6, by inserting the specific form of the fitness function and weights 1, 2, one can regulate the most significant qualities for certain applications.

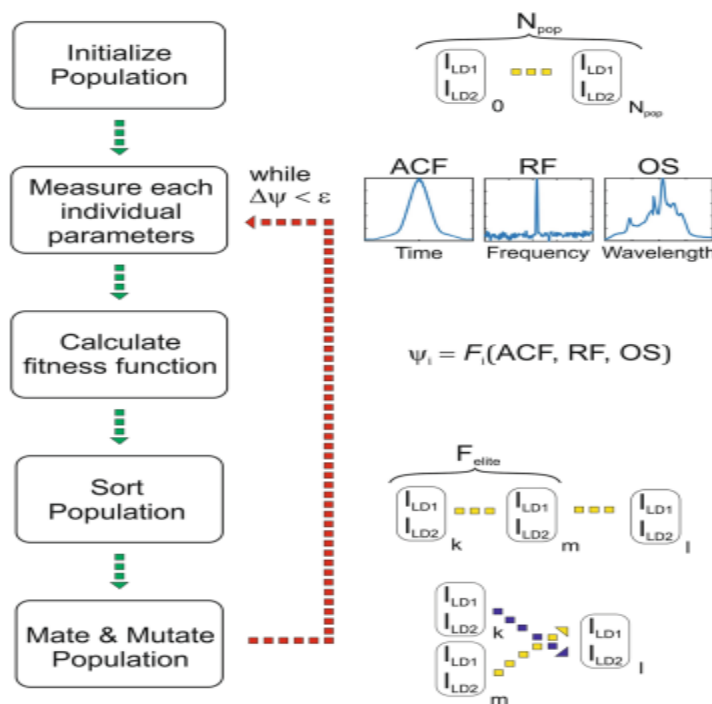
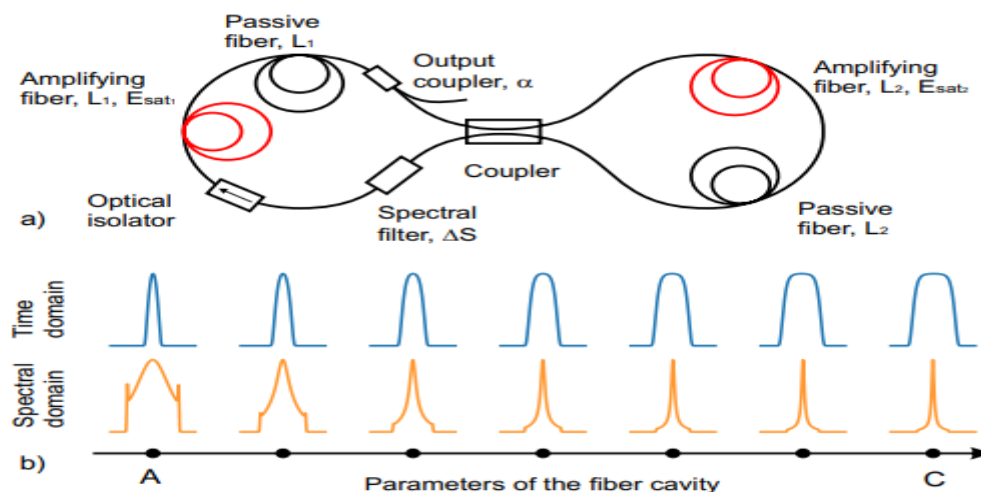


Figure 6: Particle Swarm optimization algorithm for fiber optics.

### 3. Simulation results and modelling

Recently, new methods for generating optical patterns using an electro-optical switch or a semiconductor optical amplifier it has been shown [11,12]. These techniques, on the other hand, are confined to pulse patterns that last a fraction of a second. The interaction of chromatic dispersion and Kerr nonlinearity begins to impact the spectrum and temporal form of generated optical pulses when it comes to ultra-short pulses. In the construction of classical solitons, for example, the balance condition between chromatic dispersion and nonlinearity is strictly observed. As a result, as illustrated in figure 7, the soliton fiber laser produces pulses with a limited range of temporal length and spectral width



#### Simulation result :

The mode-locked fibre laser cavity in the shape of a figure-eight is taken into account. (see Fig. 8 ). A 40/60 coupler connects two fibre rounds on the left (unidirectional) and the right (bidirectional) sides of the cavity. Both rounds of the laser resonator have amplifying portions pumped by multimode laser diodes. Only polarization-maintaining components are used in the laser cavity to avoid nonlinear polarity evolution effects. As a result, the output emission's polarization is linear. The two pump diodes' currents are controlled independently, allowing for significant variation in pulsed systems with varying output power average, contrast in radio frequency, temporal autocorrelation function, and degree of coherence. For thorough measurements of the laser, A laser control, data collection, and processing system was developed using an automated method. (see Fig. 8). the pulsed generation regimes' parameters The autocorrelation measurements were used to determine the power for diagnostics. Some

radiation is consumed in the feedback loop, and it should be confirmed that this does not influence the overall system performance. We discovered that a feedback system can be built using a laser power of 10 mW on average. Because we acquire pulses with average powers ranging from 40 to 300 milliwatts, a reduction in output power has no influence on the the output of a laser system.

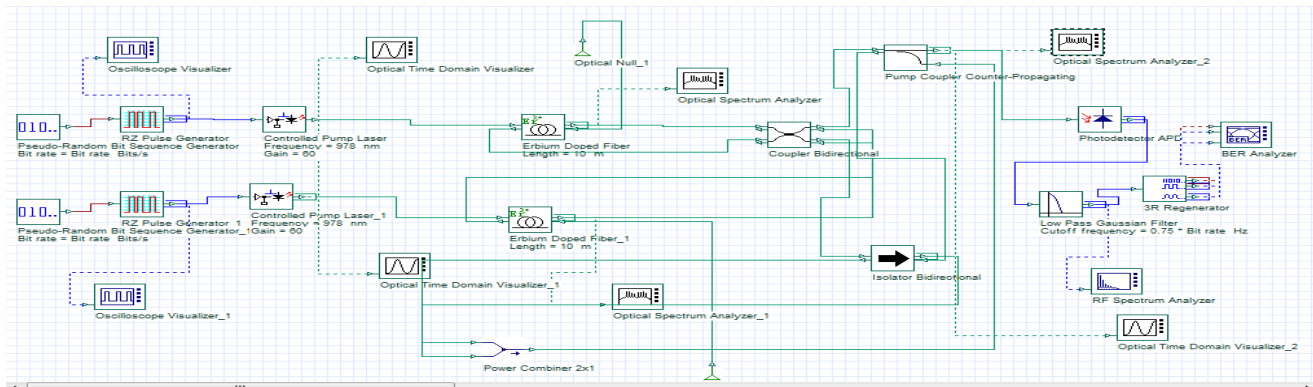


**Figure 8 : Diagram of a fiber laser with two fibers that are active stretches in both loops with optisystem**

ID1(m)	300	400	500	600	700	800
ID2(m)	300	400	500	600	700	800
FREQUENCY(nm)	1000	1000	1000	1000	1000	1000
POWER(db)	-60	-43.8	-39	-37	-35	-34
WAVELENGTH(Mm)	(1.5-1.61)	(1.5-1.61)	(1.5-1.61)	(1.5-1.61)	(1.5-1.61)	(1.5-1.61)

#### 4. Conclusions:

Machine learning is already influencing the design and optimization of photonic systems. Fiber lasers are an attractive and feasible test-bed for machine learning-based design methodologies due to their inherent complicated spatiotemporal nonlinear dynamics and concomitant high-dimensional phase space. The gradient-free PSO approach is used in this study to tackle the inverse design problem of a figure-8 fiber laser. We showed that the great variability of the pulses generated in such a system may be leveraged to generate pulses on demand with pulse lengths of 1.5 to 105 ps and spectral widths of 0.1 to 20.5 nm. The pulse parameters obtained by a number of Mode-locked fiber lasers have been studied numerically and experimentally by scientific groups such as 14,20,40, are comparable to those obtained by a number of scientific organizations using both numerical and experimental studies of mode-locked fiber lasers. Working on it, 20,41. Finally, this is the first time we've done something like this Fiber laser in the shape of an eight with all-normal dispersion and two separate amplifying fiber loops, machine learning methods are used to manage pulsed systems. This sort of laser, which features twin electronically controlled pumps, is ideal for implementing algorithm for machine learning. In one sense, within the same cavity, there are numerous conceivable lasing regimes; however, by adjusting two pumping diode currents, these operating regimes can be easily changed using electronic means. Multiple objective functions are used, as well as self-tuning adjustments to the laser cavity's two different gain levels.

#### REFERENCES

- [1] Grelu, P. & Akhmediev, N. Dissipative solitons for mode-locked lasers. *Nature Photonics* 6, 84–92 (2012).
- [2] Wise, F., Chong, A. & Renninger, W. High-energy femtosecond fiber lasers based on pulse propagation at normal dispersion. *Laser & Photonics Reviews* 2, 58–7
- [3] Fu, W., Wright, L. G., Sidorenko, P., Backus, S. & Wise, F. W. Several new directions for ultrafast fiber lasers. *Optics Express* 26, 9432–946
- [4] Turitsyn, S. K., Bale, B. G. & Fedoruk, M. P. Dispersion-managed solitons in fiber systems and lasers. *Physics Reports* 521, 135–20
- [5] Bale, B., Okhitnikov, O. & Turitsyn, S. *Modeling and Technologies of Ultrafast Fiber Lasers* 135–175 (Wiley, Hoboken, 2012).
- [6] Kim, J. & Song, Y. Ultralow-noise mode-locked fiber lasers and frequency combs: principles, status, and applications. *Adv. Opt. Photon.* 8, 465–540. <https://doi.org/10.1364/AOP.8.000465> (2016).
- [7] Chernysheva, M. et al. Carbon nanotubes for ultrafast fiber lasers. *Nanophotonics* 6, 1–30. <https://doi.org/10.1515/nanoph-2015-0156> (2017).
- [8] Baumeister, T., Brunton, S. L. & Kutz, J. N. Deep learning and model predictive control for self-tuning mode-locked lasers. *JOSA B* 35, 617–626. <https://doi.org/10.1364/JOSAB.35.000617> (2018).
- [9] Chang, G. & Wei, Z. Ultrafast fiber lasers: an expanding versatile toolbox. *iScience* 23, 101101. <https://doi.org/10.1016/j.isci.2020.101101> (2020).
- [10] Shtyrina, O. V., Yarutkina, I. A., Skidin, A., Fedoruk, M. P. & Turitsyn, S. K. Impact of the order of cavity elements in all-normal dispersion ring fiber lasers. *IEEE Photonics J.* 7, 1–7. <https://doi.org/10.1109/JPHOT.2015.2413591> (2015).
- [11] Nyushkov, B. N., Kobtsev, S. M., Ivanenko, A. V. & Smirnov, S. V. Programmable optical waveform generation in a mode-locked gain-modulated SOA-fiber laser. *JOSA B* 36, 3133–3138 (2019).

- [12] Nyushkov, B., Ivanenko, A., Smirnov, S., Shtyrina, O. & Kobtsev, S. Triggering of different pulsed regimes in fiber cavity laser by a waveguide electro-optic switch. *Opt. Express* 28, 14922–14932 (2020).
- [13] Kelly, S. Characteristic sideband instability of periodically amplified average soliton. *Electron. Lett.* 28, 806–807 (1992).
- [14] Renninger, W. H., Chong, A. & Wise, F. W. Area theorem and energy quantization for dissipative optical solitons. *JOSA B* 27, 1978–1982 (2010).
- [15] Finot, C. & Boscolo, S. *Pulse Generation and Shaping Using Fiber Nonlinearities* 115 (Wiley, Hoboken, 2017).
- [16] Kuse, N., Jiang, J., Lee, C.-C., Schibli, T. & Fermann, M. All polarization-maintaining Er fiber-based optical frequency combs with nonlinear amplifying loop mirror. *Opt. Express* 24, 3095–3102 (2016).
- [17] Aguergaray, C., Hawker, R., Runge, A. F., Erkintalo, M. & Broderick, N. G. 120 fs, 4.2 nJ pulses from an all-normal-dispersion, polarization-maintaining, fiber laser. *Appl. Phys. Lett.* 103, 121111 (2013).
- [18] Semaan, G. et al. 10  $\mu$ J dissipative soliton resonance square pulse in a dual amplifier figure-of-eight double-clad Er: Yb mode-locked fiber laser. *Opt. Lett.* 41, 4767–4770 (2016).
- [19] Kokhanovskiy, A., Ivanenko, A., Kobtsev, S., Smirnov, S. & Turitsyn, S. Machine learning methods for control of fiber lasers with double gain nonlinear loop mirror. *Sci. Rep.* 9, 1–7 (2019).
- [20] Li, D. et al. Characterization and compression of dissipative-soliton-resonance pulses in fiber lasers. *Sci. Rep.* 6, 23631 (2016).
- [21] Smirnov, S. et al. Layout of NALM fiber laser with adjustable peak power of generated pulses. *Opt. Lett.* 42, 1732–1735 (2017).
- [22] Kobtsev, S., Ivanenko, A., Kokhanovskiy, A. & Smirnov, S. Electronic control of different generation regimes in mode-locked all-fiber F8 laser. *Laser Phys. Lett.* 15, 045102 (2018).
- [23] Boscolo, S., Finot, C., Gukov, I. & Turitsyn, S. K. Performance analysis of dual-pump nonlinear amplifying loop mirror modelocked all-fiber laser. *Laser Phys. Lett.* 16, 065105 (2019).

